

https://doi.org/10.1070/QEL17244

Relaxation oscillations in a bipolarised Nd:YAG laser with a Fabry–Perot cavity

P.A. Khandokhin

Abstract. **Based on the model of a bipolarised laser, which takes into account real orientations of absorbing and emitting dipoles of active centres in the unit cell of an Nd:YAG single crystal, we have shown that the appearance of low-frequency relaxation oscillations requires the participation of both competing pump channels through linearly and circularly polarised dipole transitions.**

Keywords: *laser, polarisation mode, induced gain anisotropy, relaxation oscillations.*

1. Introduction

When the amplitude anisotropy of a cavity is low, a bipolarisation generation regime is observed, as a rule. The possibility of generation at orthogonally polarised modes contributes to the solution of various fundamental and applied problems. In particular, the study of generation peculiarities of such bipolarised lasers is attractive from the point of view of their potential application in telecommunications, data encoding, spectroscopy, etc. [1]. An integral feature of solid-state lasers is relaxation oscillations, which appear in experiments as resonance peaks at their frequencies in the spectra of intensity fluctuations of both polarisation modes and total radiation intensity [2–5]. Relaxation oscillations are subdivided into in-phase and anti-phase oscillations [6]. Low-frequency anti-phase relaxation oscillations are visible only in the spectra of intensity fluctuations of polarisation modes. When registering the total intensity, these oscillations are compensated for and are almost unobservable [4]. In-phase relaxation oscillations are visible in the spectra of both individual modes and total intensity.

The study of relaxation oscillations makes it possible to investigate the stability of the steady-state regime of generation and to predict the conditions for the loss of stability and the occurrence of an unsteady regime. All this indicates the importance of studying the influence of the interaction of polarisation modes on the lasing dynamics and on the spectrum of relaxation oscillations [7].

2. Model of an Nd:YAG laser with linearly polarised pumping

Milovskii and Khandokhin [8] proposed a model of a bipolar Nd:YAG laser based on a Fabry–Perot cavity, in which interactions with a linearly polarised pump field and fields of elliptically polarised orthogonal modes are described by taking into account the real polarisation properties of resonance transitions of nine different groups of active ions in a unit cell of a crystal matrix. The symmetry of these states is schematically shown in Fig. 1, where p_i, q_i, and r_i ($i = 1, 2, 3$) denote local orthogonal C_2-symmetry axes [9, 10]. The dipole moments of absorbing and emitting transitions are oriented along these axes in accordance with the selection rules for magnetic and electric dipole transitions [11, 12]. A model with [100] crystal orientation and polarised light of a pump laser is considered

$$\boldsymbol{E}_{\rm p} = (1/2)|\boldsymbol{E}_{\rm p}|(\boldsymbol{y}^0\cos\Psi_{\rm p} + \boldsymbol{z}^0\sin\Psi_{\rm p}) \times\exp(\mathrm{i}\omega_{\rm p}t) + \text{c.c.}, \quad (1)$$

directed along the cavity axis, which coincides with the crystallographic axis X. It is assumed that single-frequency lasing occurs on two orthogonally polarised longitudinal modes of the cavity,

$$\boldsymbol{E} = (1/2)(E_1\boldsymbol{U}_1 + E_2\boldsymbol{U}_2)\exp(\mathrm{i}\omega t) + \text{c.c.}, \quad (2)$$

having the same spatial field structure

$$\boldsymbol{U}_m = \sqrt{2}\,\boldsymbol{e}_m^0\cos kx, \quad (3)$$

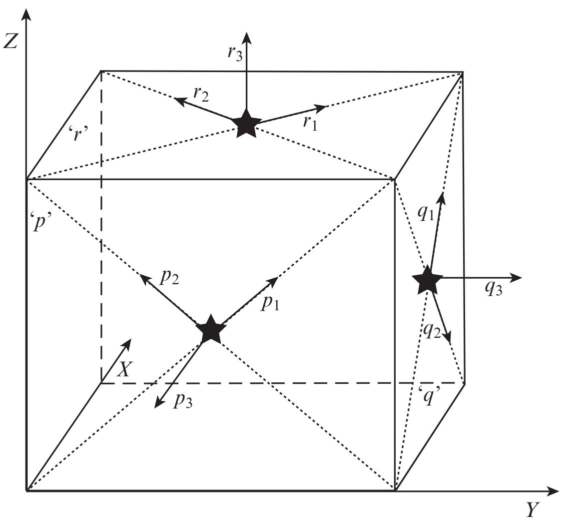

Figure 1. Possible positions of active Nd^{3+} ions (denoted by an asterisk) in the unit cell of the crystal matrix of yttrium aluminium garnet (YAG).

P.A. Khandokhin Institute of Applied Physics, Russian Academy of Sciences, ul. Ul'yanova 46, 603950 Nizhny Novgorod, Russia; e-mail: khando@appl.sci-nnov.ru

Received 13 January 2020; revision received 15 April 2020
Kvantovaya Elektronika **50** (9) 826–829 (2020)
Translated by I.A. Ulitkin

and orthogonal unit vectors $\boldsymbol{e}_m^0$ of the two eigenpolarisations

$$(\boldsymbol{e}_1^0 \cdot \boldsymbol{e}_2^{0*}) = (\boldsymbol{e}_1^{0*} \cdot \boldsymbol{e}_2^0) = 0.$$

Here $E_{1,2}$ are slowly varying complex amplitudes of orthogonally polarised fields; and ω is the carrier frequency of the generated oscillations. Each unit vector $\boldsymbol{e}_{1,2}^0$ in the general case can be represented as the sum of two projections onto the $\boldsymbol{y}^0$ and $\boldsymbol{z}^0$ directions of the principal axes of the ellipses of the laser field eigenpolarisations,

$$\boldsymbol{e}_1^0 = \boldsymbol{y}^0 \cos\theta + \mathrm{i}\boldsymbol{z}^0 \sin\theta, \tag{4}$$

$$\boldsymbol{e}_2^0 = \mathrm{i}\boldsymbol{y}^0 \sin\theta + \boldsymbol{z}^0 \cos\theta, \tag{5}$$

in which the angle θ determines the ellipticity parameter of the polarisation modes $\varepsilon = |\tan\theta|^2$.

The lasing dynamics of a bipolarised laser can be described by the system of equations [8]:

$$\frac{\mathrm{d}E_m}{\mathrm{d}\tau} = \mathrm{i}(-1)^m \delta E_m - \frac{G}{2}E_m + \frac{G}{L}\sum_s \int_x \left[(\boldsymbol{e}_{\mathrm{las}}^{\sigma_+ s}\boldsymbol{E})N_+^s(\boldsymbol{e}_{\mathrm{las}}^{\sigma_+ s}\boldsymbol{U}_m)^*\right.$$

$$\left. + (\boldsymbol{e}_{\mathrm{las}}^{\sigma_- s}\boldsymbol{E})N_-^s(\boldsymbol{e}_{\mathrm{las}}^{\sigma_- s}\boldsymbol{U}_m)^*\right]\mathrm{d}x, \; m = 1, 2, \tag{6}$$

$$\frac{\partial N_\pm^s}{\partial \tau} = gA_s - N_\pm^s\left[1 + |(\boldsymbol{e}_{\mathrm{las}}^{\sigma_\pm s}\boldsymbol{E})|^2\right]$$

$$s = p_1, p_2, p_3, q_1, q_2, q_3, r_1, r_2, r_3,$$

where

$$A_s \equiv A_s^\pi + \frac{1}{2}(A_s^{\sigma_+} + A_s^{\sigma_-}) = \frac{b_1|(\boldsymbol{e}_{\mathrm{p}}^0\boldsymbol{e}_{\mathrm{a}}^{\pi s})|^2}{b_1|(\boldsymbol{e}_{\mathrm{p}}^0\boldsymbol{e}_{\mathrm{a}}^{\pi s})|^2 + 1}$$

$$+\frac{1}{2}\left[\frac{b_2|(\boldsymbol{e}_{\mathrm{p}}^0\boldsymbol{e}_{\mathrm{a}}^{\sigma_+ s})|^2}{b_2|(\boldsymbol{e}_{\mathrm{p}}^0\boldsymbol{e}_{\mathrm{a}}^{\sigma_+ s})|^2 + 1} + \frac{b_2|(\boldsymbol{e}_{\mathrm{p}}^0\boldsymbol{e}_{\mathrm{a}}^{\sigma_- s})|^2}{b_2|(\boldsymbol{e}_{\mathrm{p}}^0\boldsymbol{e}_{\mathrm{a}}^{\sigma_- s})|^2 + 1}\right]. \tag{7}$$

Here $\tau = t/T_1$; $G = T_1/T_{\mathrm{c}}$; $g = T_1/\tau_2$; T_1, T_{c}, and τ_2 are the lifetimes of the population inversion, the field in the cavity, and the upper level of the absorbing transition, respectively; $\delta = (\omega_{\mathrm{c}}^{(1)} - \omega_{\mathrm{c}}^{(2)})T_1$; $\omega_{\mathrm{c}}^{(1),(2)}$ are the eigenfrequencies of the polarisation modes, which coincide in the absence of phase anisotropy of the cavity;

$$b_1 = b_1^0 A = \frac{\tau_2 T_{\mathrm{a}}^\pi |\mu_{\mathrm{a}}^\pi|^2}{\hbar^2}\mathrm{Re}(L_{\mathrm{a}}^\pi)|E_{\mathrm{p}}|^2;$$

$$b_2 = b_2^0 A = \frac{\tau_2 T_{\mathrm{a}}^\sigma |\mu_{\mathrm{a}}^{\sigma_\pm}|^2}{\hbar^2}\mathrm{Re}(L_{\mathrm{a}}^{\sigma_\pm})|E_{\mathrm{p}}|^2; \tag{8}$$

$A = |E_{\mathrm{p}}|^2$ is the pump parameter; $L_{\mathrm{a}}^{\pi,\sigma_\pm} = \left[1 - \mathrm{i}(\omega_{\mathrm{p}} - \omega_{\mathrm{a0}}^{\pi,\sigma_\pm})T_{\mathrm{a}}^{\pi,\sigma_\pm}\right]^{-1}$; $\mu_{\mathrm{a}}^{\pi,\sigma_\pm}$, $\omega_{\mathrm{a0}}^{\pi,\sigma_\pm}$, and $(T_{\mathrm{a}}^{\pi,\sigma_\pm})^{-1}$ are the dipole moments of transitions, centre frequencies and halfwidths of homogeneous absorption lines of the corresponding transitions; and ω_{p} is the pump laser radiation frequency. Expressions for the unit vectors of linearly and circularly polarised dipole moments of absorbing transitions of active centres located in the 'p', 'q' and 'r' faces (Fig. 1) can be found in [8].

3. Results of numerical simulation and their comparison with experimental data

System (6) describes all the features of the low-frequency dynamics of solid-state lasers with linearly polarised laser pumping. The study of the dynamic behaviour of the laser begins with finding a stationary solution to system (6) and analysing the behaviour of the image point on the phase plane when the variables deviate from the stationary state. Linearization of the system in the vicinity of a stationary state allows one to find its eigenvectors, the complex conjugate eigenvalues,

$$\lambda_j^\pm = \delta_j \pm \mathrm{i}\Omega_j, \quad j = 1, 2, 3,$$

characterising relaxation oscillations, as well as several negative real roots λ_k ($k = 1-6$) of the characteristic equation. The negativity of the real parts of the complex conjugate eigenvalues indicates that this stationary state is stable: the amplitude of any small perturbation decays exponentially. In this case, the process of relaxation to an equilibrium state is of an oscillatory nature. The imaginary part of the complex conjugate eigenvalues Ω_j determines the frequency of these relaxation oscillations, and the decrement δ_j is the rate of their decay.

Figure 2 shows the dependences of laser mode intensities, frequencies and decrements of relaxation oscillations on the pump parameter A with the participation of different absorbing dipoles. As noted above, the spectrum of relaxation oscillations can be divided into two groups: in-phase relaxation oscillation $\{\Omega_1, \delta_1\}$ and relaxation oscillations $\{\Omega_2, \delta_2\}$ and $\{\Omega_3, \delta_3\}$, caused by polarisation interaction of modes and responsible for the anti-phase behaviour of orthogonally polarised modes. In Fig. 2a, the pumping process is dominated by circularly polarised dipoles ($b_1 \neq 0$, $b_2 \neq 0$, but $b_2 \gg b_1$). For the chosen orientation of the pump polarisation ($\Psi_{\mathrm{p}} = 0$), due to the induced gain anisotropy, the intensity of the first mode I_1 significantly exceeds the intensity of the second mode I_2. In Fig. 2b, the main role is assigned to linearly polarised dipoles ($b_1 \gg b_2$), which are orthogonal to circularly polarised dipoles. In this case, the second mode has the advantage: $I_2 \gg I_1$. In both cases, an increase in the pump parameter leads to an instability of the stationary regime caused by the Hopf bifurcation at the frequency of the relaxation oscillation $\{\Omega_3, \delta_3\}$: at $A \geqslant A_{\mathrm{cr}}$, the decrement $\delta_3 \geqslant 0$ and the relaxation oscillations from decaying ones turn into undecaying self-modulation oscillations at the frequency $\Omega_m \approx \Omega_3$ [8]. As noted in this work, the instability is due to the competitive interaction of two pump channels, each of which supports an orthogonal polarisation mode. Switching off one of the competing channels leads to almost radical changes in the spectrum of relaxation oscillations and in the dynamic behaviour of the laser. Under purely single-channel excitation of the active medium, low-frequency relaxation oscillations $\{\Omega_2, \delta_2\}$ and $\{\Omega_3, \delta_3\}$ either do not appear at all ($b_2 = 0$, Fig. 3b), or appear at a high pump level ($b_1 = 0$, Fig. 3a). In this case, the steady-state lasing regime remains stable at any pump levels.

Comparison of the results of numerical simulation and experimental studies of the low-frequency dynamics of solid-state lasers [9, 10] allows us to conclude that for a correct

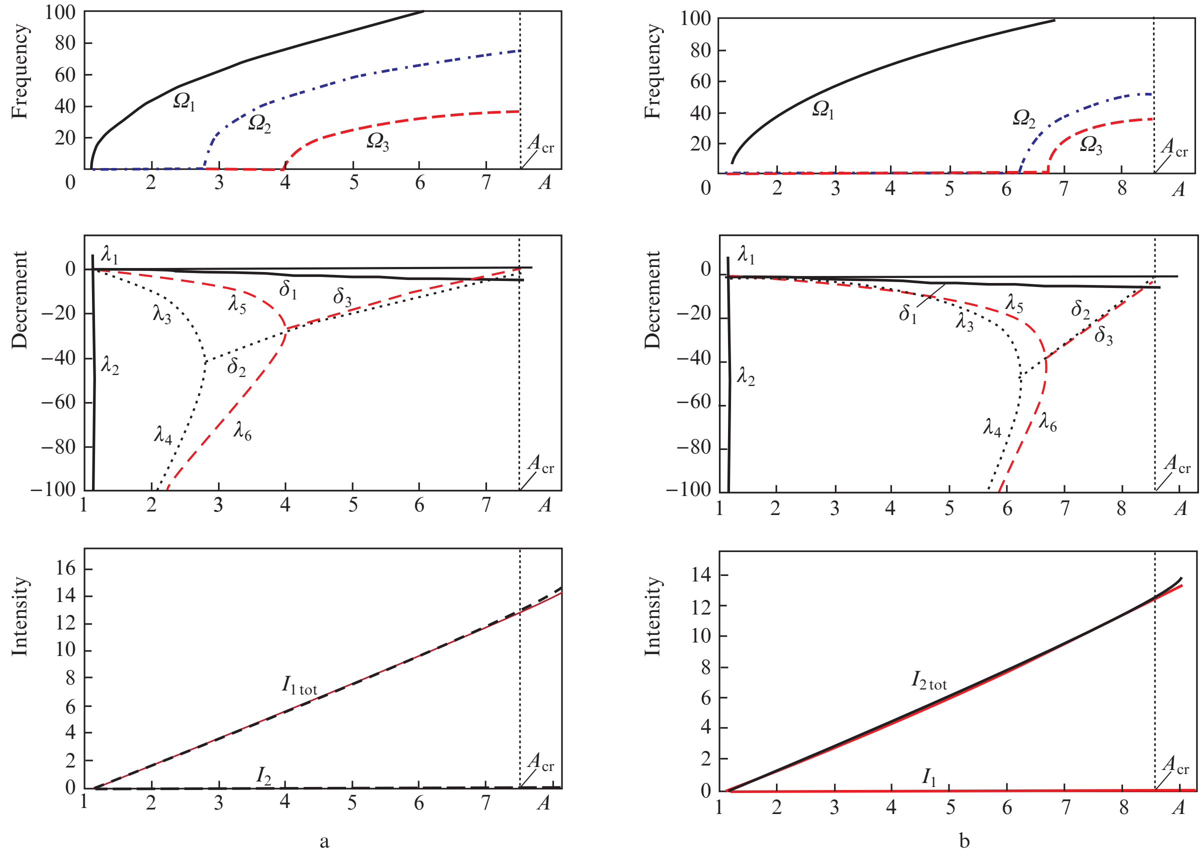

Figure 2. Intensities of laser modes, frequencies and decrements of relaxation oscillations as functions of the pump parameter A with the participation of different absorbing dipoles and $G = 1000$, $A = 5$, $\Psi_p = 0$, $\theta = 0$; (a) $b_1 = 0.0001$, $b_2 = 0.0022$ and (b) $b_1 = 0.0022$, $b_2 = 0.0001$.

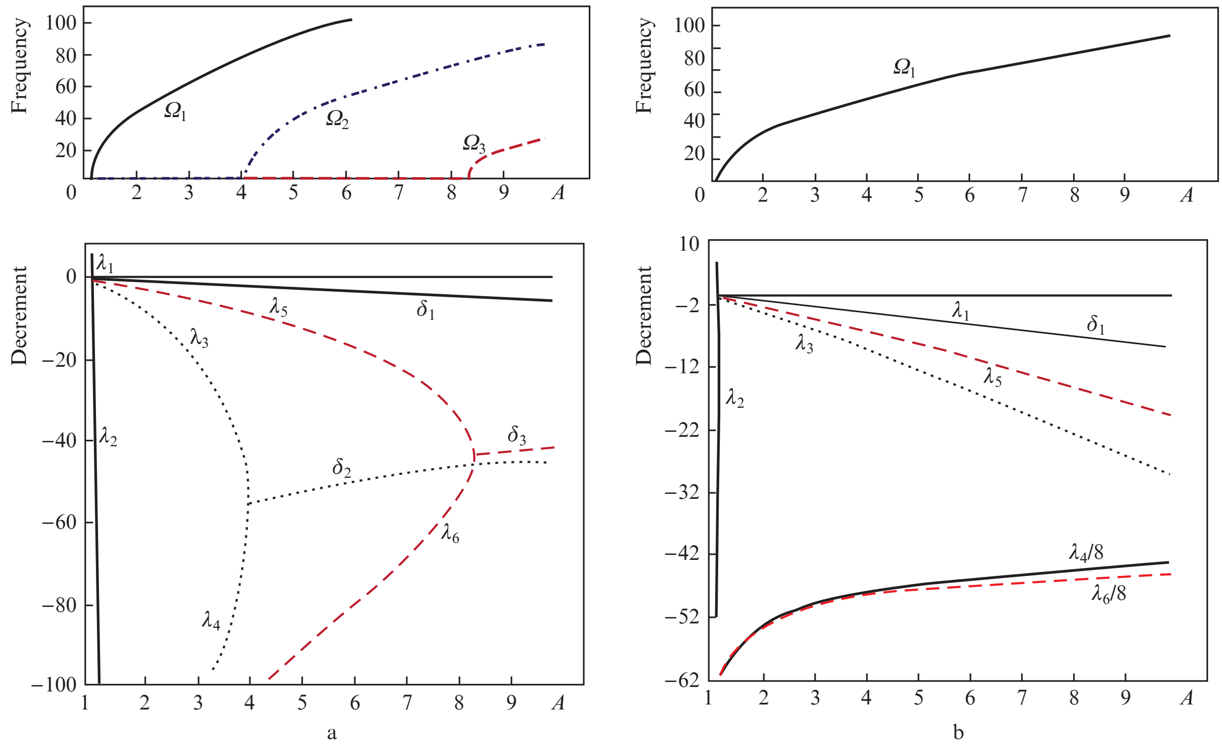

Figure 3. Frequencies and decrements of relaxation oscillations as functions of the pump parameter A for a purely single-channel type of pumping and $G = 1000$, $A = 5$, $\Psi_p = 0$, $\theta = 0$; (a) $b_1 = 0$, $b_2 = 0.0022$ and (b), $b_1 = 0.0022$, $b_2 = 0$.

description of the dynamics of Nd : YAG lasers, both pump channels must be taken into account. Only in this case (see Fig. 2), as in the experiment, all three types of relaxation oscillations are observed: in-phase relaxation oscillations $\{\Omega_1, \delta_1\}$ and anti-phase relaxation oscillations $\{\Omega_2, \delta_2\}$ and $\{\Omega_3, \delta_3\}$.

Thus, the model of a bipolarised Nd : YAG laser presented in [8], which takes into account real orientations of absorbing and emitting dipoles of active centres in the unit cell of a single crystal, made it possible to elucidate the conditions for the appearance of low-frequency relaxation oscillations. It is shown that this requires the participation of both competing pump channels through linearly and circularly polarised dipole transitions.

Acknowledgements. This work was supported within the framework of the State Assignment of the Institute of Applied Physics of the Russian Academy of Sciences (Project No. 00352014-0018).

References

1. Czarske J.W., Mueller H. *Opt. Commun.*, **114**, 223 (1995).
2. Khandokhin P.A. *Quantum Electron.*, **36**, 1161 (2006) [*Kvantovaya Elektron.*, **36**, 1161 (2006)].
3. Ievlev I.V., Khandokhin P.A., Shirokov E.Yu. *Quantum Electron.*, **36** (3) 228 (2006) [*Kvantovaya Elektron.*, **36** (3) 228 (2006)].
4. Bouwmans G., Segard B., Glorieux P., Milovsky N., Khandokhin P., Shirokov E. *Radiophys. Quantum Electron.*, **47**, 729 (2004) [*Izv. Vyssh. Uchebn. Zaved.*, *Ser. Radiofiz.*, **47**, 813 (2004)].
5. Zhang Sha., Tan Y., Zhang Shu. *J. Opt.*, **17**, 045703 (2015).
6. Khanin Ya.I. *Fundamentals of Lasers Dynamics* (Cambridge: International Science Publishing: 2006; Moscow: Nauka, 1999).
7. *Polarization Effects in Lasers and Spectroscopy*, **10** (1), (1998); **3** (2), (2001).
8. Milovskii N.D., Khandokhin P.A. *Quantum Electron.*, **49** (5), 497 (2019) [*Kvantovaya Elektron.*, **49** (5), 497 (2019)].
9. Bayerer R., Heber J., Mateika D. *Z. Phys. B*, **64**, 201 (1986).
10. San Y., Wang G.M., Cone R.L., Equall R.W., Leask M.J.M. *Phys. Rev. B*, **62**, 15443 (2000).
11. Feofilov P.P. *Usp. Fiz. Nauk*, **58**, 69 (1956).
12. Feofilov P.P., Kaplyanskii A.A. *Sov. Phys. Usp.*, **5,** 79 (1962) [*Usp. Fiz. Nauk*, **76**, 201 (1962)].